This article has been accepted for publication in IEEE Communications Letters. This is the author's version which has not been fully edited and content may change prior to final publication. Citation information: DOI 10.1109/LCOMM.2023.3264493

Solar Powered UAV-mounted RIS Networks

Yue Xiao, Dimitrios Tyrovolas, *Graduate Student Member, IEEE,* Sotiris A. Tegos, *Member, IEEE,* Panagiotis D. Diamantoulakis, *Senior Member, IEEE,* Zheng Ma, *Member, IEEE,* Li Hao, *Member, IEEE* and George K. Karagiannidis, *Fellow, IEEE*

***Abstract*—To compensate for severe blockages and achieve flexible and pervasive network access, UAV-mounted RISs have recently attracted research interest. In this work, a solar-powered UAV-mounted RIS (SUR) system is investigated, where solar cells are utilized to provide supplementary propulsion power. To maximize the energy efficiency of the SUR system, the optimal joint active and passive beamforming, as well as the energy-constrained UAV trajectory, i.e., its velocity and placement, are derived in closed form. Furthermore, subject to the size, weight, and power limitations of the UAV, the number of reflecting elements, the flying and hovering time of the SUR system are also optimized. Finally, simulations are provided to demonstrate the effectiveness of the proposed SUR system.**

***Index Terms*—unmanned aerial vehicle (UAV), reconfigurable intelligent surface (RIS), optimization, energy efficiency.**

I. Introduction

One of the most important objectives in 6G networks is the provision of seamless and ubiquitous wireless connectivity with respect to the requirements of different services [1]. However, achieving this solely via terrestrial networks may be costly and energy inefficient. In this direction, the use of unmanned aerial vehicles (UAV) to supplement the terrestrial communication systems, acting as aerial base stations (BSs), has emerged as an enabler for three-dimensional (3D) network deployment. Specifically, the advantages of aerial BSs include the flexibility of network deployment based on the traffic conditions and the required quality of service, as well as the establishment of pure line-of-sight (LoS) communication, due to the unique characteristics of aerial-to-ground links [2]. However, the use of aerial BSs is challenging, mainly due to UAV fluctuations and the corresponding stringent energy limitations, since the flight duration and communication capabilities are constrained by the limited battery capacity. [3]. Hence, a novel approach is required to further increase the energy efficiency of UAV-assisted networks and provide reliable communication regardless of any occurring UAV fluctuations.

A recently proposed idea is to control the wireless propagation phenomenon through reconfigurable intelligent surfaces (RISs) [4]. In more detail, RISs are programmable metasurfaces capable of realizing accurate manipulation of the impinging waves through the modification of their reflecting elements' reflection coefficient [5]. Therefore, by exploiting a UAV-mounted RIS, flexible 3D network coverage can be realized by placing an RIS wherever and whenever is needed [6]. In this direction, a UAV-mounted RIS-assisted network was first proposed in [7], where its superiority was shown over a terrestrial RIS-aided system, while the authors in [8] presented the benefits of UAV-mounted RISs for wireless networks due to their flexibility. Interestingly, in [9], an energy model that takes into account both UAV and RIS weights, as well as the environmental and UAV's kinematic conditions was derived, while it was proven that there exists an optimal RIS size that maximizes the number of collected data of an IoT network. Considering the time-constrained nature of UAV-assisted networks, a solar-powered UAV transmitter system was investigated in [10] to extend the UAV's flight duration. However, to the best of the authors' knowledge, no prior work has simultaneously explored the effects of RIS and solar power on a UAV-assisted system in terms of energy efficiency (EE) of a UAV-mounted RIS system, considering its unique stringent size, weight, and power (SWAP) limitations.

In this work, the utilization of a solar-powered UAV-mounted RIS (SUR) is proposed for communication purposes, where solar cells (SC) are used to provide supplemental propulsion power. In more detail, the proposed SUR system is a rotary-wing drone carrying an RIS and SC that introduces an important trade-off between communication performance and consumed energy. Specifically, the performance of the SUR-assisted system is investigated and optimized in terms of EE, while taking into account its stringent SWAP limitations. To maximize the EE, the optimal active and passive beamforming design, as well as the optimal UAV velocity and placement, are derived, while obtaining an optimal number of reflecting elements and SC area. Finally, simulations are provided to verify the accuracy of the presented analysis and demonstrate the effectiveness of a SUR-assisted system.

II. System Model

In this work, a rotary-wing UAV, denoted by R is used at a specific time instance to facilitate the information transmission from a ground BS equipped with K antennas, denoted by S, to a single-antenna ground user, denoted by D. To offer seamless connection between S and D, it is assumed that R belongs in a set of drones, which sequentially travel between two charging stations, assuring that D is continuously served by exactly one UAV. For the sake of notation simplicity, hereinafter, it is assumed that the positions of the charging stations coincide with the ones of S and D.

It should be mentioned that the considered scenario is assumed to take place in a dense urban area, leading to the

This work was supported by the European Union's Horizon 2020 research and innovation programme under grant agreement No. 957406.

Y. Xiao, Z. Ma, and L. Hao are with the Provincial Key Lab of Information Coding and Transmission, Southwest Jiaotong University, Chengdu, China (e-mails: alice_xiaoyue@hotmail.com, zma@home.swjtu.edu.cn, lhao@swjtu.edu.cn).

D. Tyrovolas, S. A. Tegos, P. D. Diamantoulakis and G. K. Karagiannidis are with the Wireless Communications and Information Processing (WCIP) Group, Electrical & Computer Engineering Department, Aristotle University of Thessaloniki, Thessaloniki, Greece (e-mails: {tyrovolas,tegosoti,padiaman,geokarag}@auth.gr). P. D. Diamantoulakis is also with the Provincial Key Lab of Information Coding and Transmission, Southwest Jiaotong University, Chengdu, China and G. K. Karagiannidis is also with the Cyber Security Systems and Applied AI Research Center, Lebanese American University (LAU), Lebanon.

neglect of any direct links between S and D due to severe terrestrial blockages. Furthermore, an RIS is mounted on the UAV, in order to turn the active transmissions into passive reflections, while SC are utilized to harvest solar energy and store it into the UAV battery, thus increasing the UAV's available energy E_B.

A. Basic assumptions

Let the number of the RIS reflecting elements be equal to N which are separated by an inter-distance d_{R}. Considering a uniform planar array RIS [11], its reflecting elements are arranged properly to create a square area (i.e., $N = M^2$) while having sub-wavelength dimensions, i.e., $s_{\mathrm{mu}} \in [\lambda/10, \lambda/2]$, where λ is the utilized wavelength. Therefore, the RIS area can be expressed as

$$\mathcal{A}_{\mathrm{RIS}} = (s_{\mathrm{mu}} + d_{\mathrm{R}})^2 M^2. \tag{1}$$

Considering the stringent SWAP limitations and the UAV aerodynamics, we set the area of the RIS equal to the SC area, i.e., $\mathcal{A}_{\mathrm{RIS}} = \mathcal{A}_{\mathrm{SC}}$. Furthermore, as the area of the SUR system is decided by the UAV's main body and the carried components (i.e., RIS, SC), the equivalent SUR area can be expressed by

$$\mathcal{A} = \max\{\mathcal{A}_{\mathrm{RIS}}, \mathcal{A}_{\mathrm{SC}}, \mathcal{S}\}, \tag{2}$$

where $\mathcal{S}$ denotes the UAV's effective area and is defined as $\mathcal{S} = \pi r^2$ with r being the rotor radius of the UAV [3].

To facilitate the path planning of the SUR-aided network, a 3D Cartesian coordinate system is utilized to specify the locations of the participating terminals, i.e., $\boldsymbol{l}_\kappa \in \mathbb{R}^{3\times 1}$ with $\kappa = \{\mathrm{S}, \mathrm{R}, \mathrm{D}\}$. Therefore, the locations of the participating nodes are assumed to be given as $\boldsymbol{l}_{\mathrm{S}} = (0, 0, 0)$, $\boldsymbol{l}_{\mathrm{R}}(t) = (x_{\mathrm{R}}, y_{\mathrm{R}}, h_{\mathrm{R}})$, and $\boldsymbol{l}_{\mathrm{D}} = (x_{\mathrm{D}}, y_{\mathrm{D}}, 0)$. It should be highlighted that the SUR location $(x_{\mathrm{R}}, y_{\mathrm{R}})$ changes over time t, within its trajectory. Therefore, the distance between two nodes can be expressed in a compact form, given by

$$d_{\kappa\kappa'} = \|\boldsymbol{l}_\kappa - \boldsymbol{l}_{\kappa'}\|, \qquad \{\kappa, \kappa'\} \in \{\mathrm{S}, \mathrm{R}, \mathrm{D}\}. \tag{3}$$

Finally, we assume that the SUR flies at an altitude h_{R} and takes a straight flight from S to D. For facilitating the presentation, the 3D coordinates of node κ can be written as $\boldsymbol{l}_\kappa = [\boldsymbol{p}_\kappa, h_\kappa]$. In more detail, it is assumed that the presented communication network is based on the fly-hover-communicate protocol, meaning that the SUR assists in the S-D communication when it starts to hover [3].

B. Signal transmission

The received signal at D via the S-R-D link, considering that the SUR is at hovering status, is given by

$$\mathrm{y}_{\mathrm{D}} = \sqrt{P_{\mathrm{s}}}\mathbf{h}_{\mathrm{RD}}^H \boldsymbol{\Theta} \mathbf{H}_{\mathrm{SR}} \mathbf{f}_{\mathrm{S}} x + n, \tag{4}$$

where P_{s}, x, and $n \in \mathcal{CN}(0, \sigma^2)$ denote the transmit power at S, the unit-power transmitted signal, and the additive white Gaussian noise with zero mean and variance σ^2, respectively. In addition, $\boldsymbol{\Theta} = \mathrm{diag}(\alpha e^{j\phi_1}, ..., \alpha e^{j\phi_N})$ denotes the induced phase shifts by the RIS with $\alpha \in [0, 1]$ and $\phi_n \in (0, 2\pi]$ being the reflection amplitude and phase shift of the n-th element, respectively. Furthermore, $\mathbf{f}_{\mathrm{S}} \in \mathbb{C}^{K\times 1}$ denotes the transmit beamforming vector with $\|\mathbf{f}_{\mathrm{S}}\|^2 = 1$ [11], while the communication channels $\mathbf{h}_{\mathrm{RD}}^H \in \mathbb{C}^{1\times N}$ and $\mathbf{H}_{\mathrm{SR}} \in \mathbb{C}^{N\times K}$, which are assumed to be LoS, can be described as

$$\begin{aligned}\mathbf{h}_{\mathrm{RD}}^H = \sqrt{g_{\mathrm{RD}}} e^{j\frac{2\pi d_{\mathrm{RD}}}{\lambda}} \left[1, \ldots, e^{j\frac{2\pi d_{\mathrm{R}}}{\lambda}(M-1)\sin(\theta_{\mathrm{D}})\cos(\omega_{\mathrm{D}})}\right] \\ \otimes \left[1, \ldots, e^{j\frac{2\pi d_{\mathrm{R}}}{\lambda}(M-1)\sin(\theta_{\mathrm{D}})\sin(\omega_{\mathrm{D}})}\right],\end{aligned} \tag{5}$$

and

$$\begin{aligned}\mathbf{H}_{\mathrm{SR}} = \sqrt{g_{\mathrm{SR}}} e^{-j\frac{2\pi d_{\mathrm{SR}}}{\lambda}} \left[1, \ldots, e^{-j\frac{2\pi d_{\mathrm{R}}}{\lambda}(M-1)\sin(\theta_{\mathrm{R}})\cos(\omega_{\mathrm{R}})}\right]^T \\ \otimes \left[1, \ldots, e^{-j\frac{2\pi d_{\mathrm{R}}}{\lambda}(M-1)\sin(\theta_{\mathrm{R}})\sin(\omega_{\mathrm{R}})}\right]^T \mathbf{a}_{\mathrm{S}}^H,\end{aligned} \tag{6}$$

where $g_{\kappa\kappa'} = \beta_0 d_{\kappa\kappa'}^{-\kappa_0}$ indicates the path loss factor with β_0 and κ_0 being the path loss at the reference distance $d_0 = 1$ m and the path loss exponent, respectively, and $\mathbf{a}_{\mathrm{S}} \in \mathbb{C}^{K\times 1}$ is the transmit array response of S with $||\mathbf{a}_{\mathrm{S}}||^2 = K$. Finally, θ_{R} and ω_{R} denote the RIS elevation and azimuth angles of arrival, θ_{D} and ω_{D} denote the RIS elevation and azimuth angles of departure. Therefore, the achievable spectral efficiency (SE) of the end-to-end SUR-assisted communication is given by

$$R = \log_2\left(1 + \frac{P_{\mathrm{s}}}{\sigma^2}\left|\mathbf{h}_{\mathrm{RD}}^H \boldsymbol{\Theta} \mathbf{H}_{\mathrm{SR}} \mathbf{f}_{\mathrm{S}}\right|^2\right) \quad \text{[bps/Hz]}. \tag{7}$$

C. Energy harvesting

By introducing SC on a UAV-mounted RIS, the flight duration can be extended. Specifically, the flight duration is a function of the power consumption which is mainly composed of two parts, i.e., the communication-related energy (i.e., RIS) and the propulsion energy cost (i.e., UAV motors) [3], [9]. It should be highlighted that the RIS power consumption comes from the reflection elements configuration circuitry, which is in the order of micro-watts, thus it can be neglected [9]. Therefore, the power consumption of a UAV-mounted RIS system is mainly affected by its flight mechanisms, thus the total available energy at the SUR system is

$$E_{\mathrm{U}} = E_{\mathrm{B}} + (T_{\mathrm{f}} + T_{\mathrm{h}})P_{\mathrm{sc}}, \tag{8}$$

where P_{sc} is the SC harvested power, which can be modeled as $P_{\mathrm{sc}} = \xi I \mathcal{A}_{\mathrm{SC}} e^{-\beta_{\mathrm{s}}}$ with ξ and I being constants indicating the SC efficiency and the solar radiation intensity, respectively. Moreover, $\beta_{\mathrm{s}} \geq 0$ represents the absorption coefficient of the clouds, which is affected by the clouds' altitude [10]. It is noted that the SC harvested energy is proportional to their area. However, SC should be designed according to the stringent SWAP limitations of the SUR system, as shown in (2).

D. SUR Power Consumption

For a rotary-wing UAV with weight w that flies with speed v, the propulsion power consumption can be modeled as [3]

$$P_{\mathrm{f}}(v) = \underbrace{\frac{w^{3/2}}{\sqrt{2\rho\mathcal{A}}}\widetilde{v}}_{\text{induced power}} + \underbrace{\frac{1}{2}C_{\mathrm{p}}v^3}_{\text{parasitic power}} + \underbrace{C_{\mathrm{b}}\left(1 + \frac{3v^2}{v_{\mathrm{r}}^2}\right)}_{\text{blade profile}}, \tag{9}$$

where $\widetilde{v} = \sqrt{\sqrt{1 + v^4/4v_0^4} - v^2/2v_0^2}$ with ρ, v_0, and v_{r} being the air density, the mean rotor induced velocity, and the tip speed of the rotor blade, respectively [3]. Additionally, $C_{\mathrm{p}} = r_0 \rho s \mathcal{A}$ and $C_{\mathrm{b}} = \frac{\sigma_{\mathrm{p}}}{8}\rho s \mathcal{A} \Omega^3 r^3$ denote the constant of

This article has been accepted for publication in IEEE Communications Letters. This is the author's version which has not been fully edited and content may change prior to final publication. Citation information: DOI 10.1109/LCOMM.2023.3264493

the parasitic status and the blade profile status, respectively, where r_0, s, $\sigma_{\rm p}$, and Ω indicate the fuselage drag ratio, the rotor solidity, the profile drag ratio, and the blade angular velocity. Furthermore, the weight of the proposed SUR system can be expressed as $w = w_{\rm u} + a_0\mathcal{A}_{\rm RIS} + b_0\mathcal{A}_{\rm SC}$, where $w_{\rm u}$, a_0, and b_0 denote the weight of the UAV, the densities per unit area for the RIS and SC, respectively. Finally, the SUR power consumption for the hovering case, i.e., $v = 0$, is equal to $P_{\rm h} = \frac{w^{\frac{3}{2}}}{\sqrt{2\rho\mathcal{A}}} + C_{\rm b}$, where it can be observed that for the hovering case, the term of parasitic power does not affect the SUR system.

III. SUR Design

The utilization of a SUR system introduces an important trade-off between communication performance and consumed energy. Specifically, as the SC and RIS areas increase, the solar harvested energy also increases, and the equivalent channel conditions enhance. However, such an increase comes with the disadvantage of larger power consumption, as the motors need to consume more power to support the flight of the SUR system due to the increased weight. Hence, the maximization of EE is expected to balance the communication performance and the UAV equipment.

In general, the energy efficient use of UAVs is a key objective in the design of UAV-assisted networks [12]. To this end, similarly to [12], we define the EE of the SUR system as the fraction of the number of bits delivered at D to the energy consumption of the SUR, i.e.,

$$\mathcal{E} = \frac{T_{\rm h}BR}{U} \quad \text{[bits/Joule]}, \tag{10}$$

where B is the channel bandwidth, BR (bits/s) is the end-to-end channel capacity, and U is the total consumed energy taking into account energy harvesting, which consists of four terms and is expressed as

$$U = \underbrace{\int_0^{T_{\rm f}} P_{\rm f}(v(t))dt + T_{\rm h}P_{\rm h} + T_{\rm h}P_{\rm circ}}_{\text{energy for flying, hovering, and RIS circuitry}} - \underbrace{(T_{\rm f}+T_{\rm h})P_{\rm sc}}_{\text{harvested energy}}. \tag{11}$$

The first two terms correspond to the energy dissipation needed for the SUR flying and hovering, while the last term represents the harvested energy. Furthermore, $P_{\rm circ} = NP_n + P_c$ denotes the power consumption of the RIS circuitry with P_n and P_c being the consumed power by each reflecting element and the RIS controller, respectively. The minus sign in front of $(T_{\rm f}+T_{\rm h})P_{\rm sc}$ indicates that the increase of this term has a positive impact on EE, which is in line with the definition of EE used in [13].

Next, the aforementioned metric is maximized, by designing the optimal flight strategy of the SUR-assisted system, for the case where S and D have fixed locations and the fly-hover-communicate protocol is used. Specifically, we design the proposed SUR system in terms of maximizing $\mathcal{E}$ with respect to the system's active/passive beamforming, i.e., $\mathbf{f}_{\rm S}$, $\boldsymbol{\Theta}$, the optimal hovering position of the SUR, i.e., $\boldsymbol{l}_{\rm R}$, the flying speed v, the number of reflecting elements N, the flying time $T_{\rm f}$, and the hovering time $T_{\rm h}$. Thus, the aforementioned optimization problem can be expressed as

$$(\mathcal{P}1): \max_{\mathbf{f}_{\rm S},\,\boldsymbol{\Theta},\,\boldsymbol{l}_{\rm R},\,v,\,N,\,T_{\rm f},\,T_{\rm h}} \quad \mathcal{E} \tag{12}$$

$$\begin{aligned}
\text{s.t.}\quad & {\rm C}_1: \|\mathbf{f}_{\rm S}\|^2 = 1,\\
& {\rm C}_2: \phi_n \in [0, 2\pi],\ n = 1, ..., N,\\
& {\rm C}_3: x_{\rm R} \in [0, x_{\rm D}],\ y_{\rm R} \in [0, y_{\rm D}],\\
& {\rm C}_4: \int_0^{T_{\rm f}} v(t)dt = d_{\rm SD},\\
& {\rm C}_5: \int_0^{T_{\rm f}} P_{\rm f}(v(t))dt + T_{\rm h}P_{\rm h} + T_{\rm h}P_{\rm circ} = E_{\rm U},\\
& {\rm C}_6: \mathcal{A}_{\rm RIS} = \mathcal{A}_{\rm SC}.
\end{aligned}$$

Regarding $(\mathcal{P}1)$ constraints, ${\rm C}_1$ denotes the power constraint of the active beamforming design at S and D, while ${\rm C}_2$ describes the angle constraint of the reflection phase at R. Furthermore, ${\rm C}_3$ and ${\rm C}_4$ express the SUR departure and arrival locations and the SUR traveling distance, while ${\rm C}_5$ ensures that the SUR system utilizes the available energy to complete its mission and land at D. Moreover, by substituting (8) into ${\rm C}_5$, it is evident that $\mathcal{E}$ is always non-negative and can be maximized when $U = E_{\rm B}$. Finally, ${\rm C}_6$ restricts the size of the SC and RIS, due to the SWAP limitations of the SUR system.

Thus, considering the uncoupled variables, the multi-variable optimization problem $(\mathcal{P}1)$ with given $d_{\rm SD}$ can be solved by dividing it into the following disjoint sub-problems: (i) in $(\mathcal{P}1.1)$, the maximal SE can be obtained with the optimal active and passive beamforming, i.e., $\mathbf{f}_{\rm S}$, $\boldsymbol{\Theta}$ constrained by ${\rm C}_1$ and ${\rm C}_2$, respectively, (ii) in $(\mathcal{P}1.2)$, the optimal hovering position of the SUR is obtained constrained by ${\rm C}_3$, and (iii) in $(\mathcal{P}1.3)$, the SUR flying speed and the number of reflecting elements can be optimized, with respect to ${\rm C}_4$, ${\rm C}_5$ and ${\rm C}_6$ for fixed S and D locations. The corresponding solutions are provided in the following subsections.

A. Joint Active & Passive Beamforming Design

By setting $U = E_{\rm B}$, the optimization problem $(\mathcal{P}1)$ with respect to the optimal beamforming design can be transformed to the SE maximization problem, i.e.,

$$\begin{aligned}
(\mathcal{P}1.1): \max_{\mathbf{f}_{\rm S},\,\boldsymbol{\Theta}} \quad & R\\
\text{s.t.}\quad & {\rm C}_1 - {\rm C}_2.
\end{aligned} \tag{13}$$

In this direction, the optimal active beamforming vector at S is $\mathbf{f}_{\rm S}^* = \frac{a_{\rm S}}{\sqrt{K}}$ [11], thus the optimal passive beamforming design of the SUR system is given as $\phi_n^* = -\arg\left(\left[\mathbf{h}_{\rm RD}^H\right]_n \left[\mathbf{H}_{\rm SR}\mathbf{f}_{\rm S}\right]_n\right)$. To this end, the maximal SE is

$$R^* = \log_2\left(1 + \frac{P_{\rm s}K(\alpha N\beta_0)^2}{\sigma^2\left(\|\boldsymbol{l}_{\rm S} - \boldsymbol{l}_{\rm R}\|\|\boldsymbol{l}_{\rm R} - \boldsymbol{l}_{\rm D}\|\right)^{\kappa_0}}\right). \tag{14}$$

B. SUR Optimal Hovering Position

Subsequently, based on (14), the optimal horizontal placement of the UAV leading to the minimum equivalent gain of the channel loss is given by

$$\begin{aligned}
(\mathcal{P}1.2): \min_{\boldsymbol{p}_{\rm R}} \quad & (h_{\rm R}^2 + \|\boldsymbol{p}_{\rm R} - \boldsymbol{p}_{\rm D}\|^2)(h_{\rm R}^2 + \|\boldsymbol{p}_{\rm R} - \boldsymbol{p}_{\rm S}\|^2)\\
\text{s.t.}\quad & {\rm C}_3.
\end{aligned} \tag{15}$$

Hence, a closed-form expression for the optimal location of the SUR is provided in the following proposition.

Proposition 1. *The optimal horizontal position of the presented SUR system is given by*

$$\boldsymbol{p}_{\mathrm{R}}^{*}=\left[\frac{1}{2}\pm\sqrt{\max\left(\frac{1}{4}-\left(\frac{h_{\mathrm{R}}}{\|\boldsymbol{p}_{\mathrm{D}}\|}\right)^{2},0\right)}\right]\boldsymbol{p}_{\mathrm{D}}. \tag{16}$$

Proof: The proof can be omitted, since similar steps are followed in [11]. ■

C. SUR Trajectory Design

By taking into account the binary flying status of the SUR in the fly-hover-communication protocol, $(\mathcal{P}1)$ with $U=E_{\mathrm{B}}$ can be transformed into the maximization problem of the EE when the SUR is in hovering status. Specifically, the aforementioned problem can be expressed as

$$\begin{aligned}(\mathcal{P}1.3):\ &\max_{N,\,v,\,T_{\mathrm{f}},\,T_{\mathrm{h}}}\quad T_{\mathrm{h}}R^{*}\\ &\text{s.t.}\quad \mathrm{C}_4-\mathrm{C}_6.\end{aligned} \tag{17}$$

Proposition 2. *The optimal moving strategy for maximizing the EE can be achieved with constant speed flight v. For the optimal flying time, from C_4, $T_{\mathrm{f}}^{*}=\frac{d_{\mathrm{SD}}}{v}$ and, considering C_5, the optimal hovering time is given by*

$$T_{\mathrm{h}}^{*}=\frac{E_{\mathrm{B}}+\left(P_{\mathrm{sc}}-P_{\mathrm{f}}(v)\right)\frac{d_{\mathrm{SD}}}{v}}{P_{\mathrm{h}}+P_{\mathrm{circ}}-P_{\mathrm{sc}}}, \tag{18}$$

when $E_{\mathrm{B}}+\left(P_{\mathrm{sc}}-P_{\mathrm{f}}(v)\right)\frac{d_{\mathrm{SD}}}{v}>0$ and $(P_{\mathrm{h}}+P_{\mathrm{circ}}-P_{\mathrm{sc}})>0$.

Proof: C_5 can be further expressed as

$$\begin{aligned}T_{\mathrm{h}}(P_{\mathrm{h}}+P_{\mathrm{circ}}-P_{\mathrm{sc}})&=E_{\mathrm{B}}+T_{\mathrm{f}}P_{\mathrm{sc}}-\int_{0}^{T_{\mathrm{f}}}P_{\mathrm{f}}(v(t))dt\\ &\overset{(a)}{\leq}E_{\mathrm{B}}+T_{\mathrm{f}}P_{\mathrm{sc}}-T_{\mathrm{f}}P_{\mathrm{f}}\left(\frac{1}{T_{\mathrm{f}}}\int_{0}^{T_{\mathrm{f}}}v(t)\,dt\right),\end{aligned} \tag{19}$$

where step (a) is established by the convexity of $P_{\mathrm{f}}(v(t))$ with respect to $v(t)>0$, thus the Jensen's inequality can be leveraged, which completes the proof. ■

1) Optimal design of v with fixed N

Considering a fixed number of reflecting elements N and the constraints in Proposition 2, the optimal design of speed v can be transformed to the *minimum-energy* (ME) speed as

$$v_{\mathrm{me}}=\underset{0<v\leq v_{\max}}{\operatorname{argmin}}\ \frac{(P_{\mathrm{f}}(v)-P_{\mathrm{sc}})d_{\mathrm{SD}}}{v}. \tag{20}$$

It should be highlighted that the ME speed also denotes the SUR system propulsion energy cost per unit traveling distance [3]. Furthermore, an easily implemented approximation is preferable to obtain v_{me} in a tractable closed-form expression, as presented in the following proposition.

Proposition 3. *The optimal ME speed is decided by the non-complex and non-negative value of*

$$v_{\mathrm{me}}=\frac{-(\tilde{g}\mp k)\pm\sqrt{(\tilde{g}\mp k)^{2}-4(\frac{y_0}{2}\pm kx_0)}}{2} \tag{21}$$

where $\tilde{g}=\frac{g}{4p}$, $k=\sqrt{\frac{g^2}{9p^2}+y_0}$, and $x_0=\frac{-2(gy_0+2C_{\mathrm{b}}')p}{g^2+16y_0p^2}$ with $p=\frac{C_p}{2}$, $g=\frac{3C_{\mathrm{b}}}{v_{\mathrm{r}}^2}$, and $C_{\mathrm{b}}'=(C_{\mathrm{b}}-P_{\mathrm{sc}})$. Moreover, $y_0=(-q-\Delta)^{\frac{1}{3}}+(-q+\Delta)^{\frac{1}{3}}$, where $\Delta=\sqrt{q^2+m^3}$ with $q=\frac{fg^2-pC_{\mathrm{b}}^2}{8p^3}$, $m=\frac{16fg-gC_{\mathrm{b}}}{12p^2}$, and $f=\frac{w^{3/2}v_0}{\sqrt{2\rho\mathcal{A}}}$.

Proof: By applying the Taylor expansion, the propulsion power consumption in (9) with $v\neq 0$ can be given as

$$P_{\mathrm{f}}(v)\approx pv^3+gv^2+C_{\mathrm{b}}+hv^{-1}, \tag{22}$$

where $h=\frac{w^{3/2}v_0}{\sqrt{2\rho\mathcal{A}}}$. By substituting (22) into (20), v_{me} can be obtained by setting its first order derivative equal to zero, i.e., $2pv+g-C_{\mathrm{b}}'v^{-2}-2hv^{-3}=0$. Eventually, the proof is completed by means of the Ferrari-Cardano method [14]. ■

2) Joint Optimization of N and v

Next, the joint optimization of N and v is considered in this subsection. Specifically, by substituting (18) and (14) into $(\mathcal{P}1.3)$, the objective optimization can be transformed into a multivariate optimization problem as

$$\min_{N,\,v}\ f(N,v), \tag{23}$$

where $f(N,v)=-T_{\mathrm{h}}^{*}(N,v)R^{*}(N)$ with $N>0$ and $v>0$. Herein, (2) can be rewritten as $\mathcal{A}=\frac{|\mathcal{A}_{\mathrm{RIS}}-S|}{2}+\frac{\mathcal{A}_{\mathrm{RIS}}+S}{2}$.

First, to obtain the optimal variables in (23), a direct solution is to let the partial derivation as $\nabla_N f(N,v)$ and $\nabla_v f(N,v)$. Although $f(N,v)$ is differentiable over N and v, it is still hard to obtain the closed-form expression for the stationary points corresponding to $\nabla_N f(N,v)=0$ and $\nabla_v f(N,v)=0$. Thus, to tackle this unconstrained non-convex problem and mitigate persistent oscillations of the conventional gradient descent scheme, a momentum term can be introduced to accumulate the gradients from previous iterations and accelerate the training in a more relevant direction. Therefore, it stands

$$d_N^{(i+1)}=\gamma d_N^{(i)}+\nabla f_N(N,v^{(i)}), \tag{24}$$

$$N^{(i+1)}=N^{(i)}-\eta d_N^{(i+1)}, \tag{25}$$

$$d_v^{(i+1)}=\gamma d_v^{(i)}+\nabla f_v(N^{(i)},v), \tag{26}$$

$$v^{(i+1)}=v^{(i)}-\eta d_v^{(i)} \tag{27}$$

with $d_N^{(i+1)}$ and $d_v^{(i+1)}$ being the momentum term. Also, γ is the momentum-related attenuation factor and η denotes the learning rate. Based on the above steps, an overall diagram of the solution to $(\mathcal{P}1)$ is summarized in Algorithm 1.

Lemma 1. *With $i\to\infty$, the sequence $\{N^{(i)},v^{(i)}\}$ generated by the momentum gradient descent (MGD) converges to a stationary point $\{N^{*},v^{*}\}$ of problem $(\mathcal{P}1.3)$.*

Proof: First, $f(N,v)$ in $(\mathcal{P}1.3)$ is non-convex but differentiable over N and v in its feasible region. With fixed N, for $\{v_1,v_2\}\in(0,v_{\max}]$, there exists $L_1>0$ to meet $|\nabla_v f(N,v_1)-\nabla_v f(N,v_2)|\leq L_1|v_1-v_2|$ and a similar result for N can be extracted by fixing $v\in\mathcal{S}$. Thus, the gradient of $f(N,v)$ in $(\mathcal{P}1.3)$ is Lipschitz continuous in its bounded region, hence, according to the Lyapunov direct method utilized in [15], the sequence $\{N^k,v^k\}$ generated by the MGD converges to a stationary point. ■

IV. Simulation

In this section, numerical results for the SUR system are provided to validate the effectiveness of SC, considering the UAV-mounted RIS system without SC as a benchmark. Unless otherwise stated, the system parameters are given in Table I.

In Fig. 1, assuming that $\mathcal{A}_{\mathrm{SC}}=\mathcal{S}$, the energy consumption for the SUR flight, i.e., $(P_{\mathrm{f}}-\tau P_{\mathrm{sc}})/v$, versus its horizontal speed v is plotted. For ease of description, we indicate $\Delta P_{\mathrm{f}}=P_{\mathrm{f}}-\tau P_{\mathrm{sc}}$ in the figure, where $\tau=\{0,1\}$ indicates the cases without (wo.) or with (w.) SC, respectively. As it can be

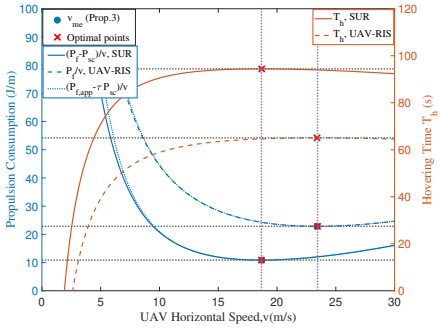

Fig. 1: Propulsion consumption versus UAV speed.

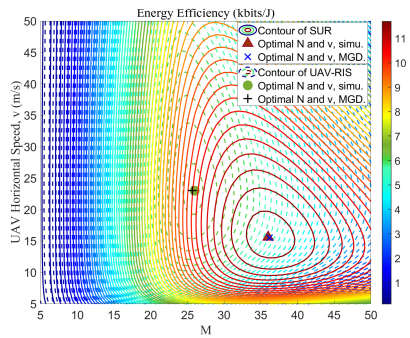

Fig. 2: Contour plot of EE.

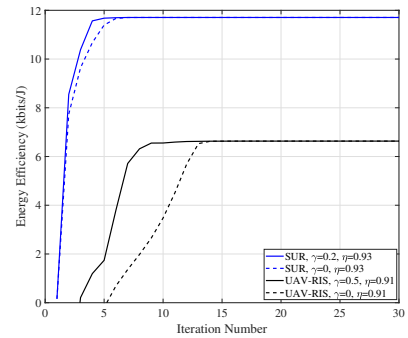

Fig. 3: EE versus iteration number.

Algorithm 1 SUR Design

Input: K, a_{S}, d_{SD}, $\mathbf{h}_{\mathrm{RD}}^H$, $\mathbf{H}_{\mathrm{SR}}$ $N^{(0)}$, $v^{(0)}$ and $i=0$;
Output: $\mathcal{E}^*$;
update $\mathbf{f}_{\mathrm{S}}^* = \frac{\mathbf{a}_{\mathrm{S}}}{\sqrt{K}}$, $\phi_n^* = -\arg\left(\left[\mathbf{h}_{\mathrm{RD}}^H\right]_n \left[\mathbf{H}_{\mathrm{SR}}\mathbf{f}_{\mathrm{S}}^*\right]_n\right)$;
update $\boldsymbol{p}_{\mathrm{R}}^*$ using (16), T_{h}^* using (18);
Repeat
  update $N^{(i+1)}$ according to (24) and (25);
  update $v^{(i+1)}$ according to (26) and (27);
  update $i \leftarrow i+1$;
Until meeting the stopping criteria.

TABLE I: Simulation parameters.

Parameter	Value	Parameter	Value	Parameter	Value
λ	0.125 m	ρ	1.225 kg/m^3	β_{s}	0.7
v_0	4.03 m/s	v_{r}	120 m/s	r	0.5 m
h_{R}	50 m	r_0	0.6	s	0.05
σ_{p}	0.012	Ω	300 rad/s	κ_0	2
P_{s}/σ^2	30 dB	E_{B}	50 kJ	ξI	0.5 $\times$ 1367 W/m^2
d_{R}	$\lambda/10$	s_{mu}	$\lambda/5$	α	1
w_{u}	50 N	a_0	30 N/m^2	b_0	10 N/m^2
β_0	2	K	16	B	1 MHz
P_n	2 μW	P_c	50 mW		

observed, the calculated power consumption in (22) approximates well the actual power consumption, especially for larger v values. To find the speed that achieves the minimum energy consumption as shown in (20), an exhaustive search of v_{me} is performed to verify the accuracy of Proposition 3. Moreover, considering the effect of SC, at the same flight speed, the SUR can provide communication for a longer duration and consume less propulsion energy compared with the UAV-mounted RIS case. Specifically, taking the optimal UAV speed, the effect of SC in the SUR system can save the propulsion consumption by approximately 30%, while the communication time can be almost doubled. Also, two auxiliary lines are plotted to demonstrate that the obtained v_{me} corresponds to the maximum T_{h}, which further explores the relationship between Propositions 2 and 3.

Regarding the joint optimization of the reflecting elements and the UAV speed, which aims at maximizing the EE within the UAV's trajectory, Fig. 2 is presented to illustrate the joint effect of N and v on $T_{\mathrm{h}}^* R^*$ for the cases of a SUR system. It can be observed that compared with the UAV-mounted RIS, a SUR system can increase the EE, since additional energy is provided through the mounted SC which can support the utilization of more RIS elements. Specifically, with the optimal setting, the SUR can achieve almost double EE.

To further explore the efficiency of the MGD-based algorithm, in Fig. 3, the convergence of Algorithm 1 is illustrated. Moreover, Fig. 3 illustrates the impact of γ on the convergence rate, and specifically, $\gamma = 0.4$ and presents the largest convergence rate for the SUR case, while $\gamma = 0.5$ is the optimal value for a UAV-mounted RIS.

References

[1] Z. Zhang, Y. Xiao, Z. Ma, M. Xiao, Z. Ding, X. Lei, G. K. Karagiannidis, and P. Fan, "6G wireless networks: Vision, requirements, architecture, and key technologies," *IEEE Veh. Technol. Mag.*, vol. 14, no. 3, pp. 28–41, 2019.

[2] H. Sami, R. Saado, A. E. Saoudi, A. Mourad, H. Otrok, and J. Bentahar, "Opportunistic UAV deployment for intelligent on-demand IoV service management," *IEEE Trans. Netw. Service Manag.*, pp. 1–1, 2023.

[3] Y. Zeng, J. Xu, and R. Zhang, "Energy minimization for wireless communication with rotary-wing UAV," *IEEE Trans. Wireless Commun.*, vol. 18, no. 4, pp. 2329–2345, 2019.

[4] Q. Wu, S. Zhang, B. Zheng, C. You, and R. Zhang, "Intelligent reflecting surface-aided wireless communications: A tutorial," *IEEE Trans. Commun*, vol. 69, no. 5, pp. 3313–3351, 2021.

[5] D. Tyrovolas, S. A. Tegos, P. D. Diamantoulakis, and G. K. Karagiannidis, "Synergetic UAV-RIS communication with highly directional transmission," *IEEE Wireless Commun. Lett.*, vol. 11, no. 3, pp. 583–587, 2022.

[6] D. Tyrovolas, P.-V. Mekikis, S. A. Tegos, P. D. Diamantoulakis, C. K. Liaskos, and G. K. Karagiannidis, "On the performance of HARQ in IoT networking with UAV-mounted reconfigurable intelligent surfaces," in *Proc. IEEE Vehicular Technology Conference: (VTC-Spring)*, 2022.

[7] Q. Zhang, W. Saad, and et.al., "Reflections in the sky: Millimeter wave communication with UAV-carried intelligent reflectors," in *Proc. IEEE Global Communications Conference (GLOBECOM)*, 2019, pp. 1–6.

[8] C. You, Z. Kang, Y. Zeng, and R. Zhang, "Enabling Smart Reflection in Integrated Air-Ground Wireless Network: IRS Meets UAV," *IEEE Wirel. Commun.*, vol. 28, no. 6, pp. 138–144, 2021.

[9] D. Tyrovolas, P.-V. Mekikis, S. A. Tegos, P. D. Diamantoulakis, C. K. Liaskos, and G. K. Karagiannidis, "Energy-aware design of UAV-mounted RIS networks for IoT data collection," *IEEE Trans. Commun.*, vol. 71, no. 2, pp. 1168–1178, 2023.

[10] Y. Sun, D. Xu, and et.al., "Optimal 3D-trajectory design and resource allocation for solar-powered UAV communication systems," *IEEE Trans. Commun*, vol. 67, no. 6, pp. 4281–4298, 2019.

[11] H. Lu, Y. Zeng, and et.al., "Aerial intelligent reflecting surface: Joint placement and passive beamforming design with 3D beam flattening," *IEEE Trans. Wirel. Commun.*, vol. 20, no. 7, pp. 4128–4143, 2021.

[12] Y. Zeng and R. Zhang, "Energy-efficient UAV communication with trajectory optimization," *IEEE Trans. Wireless Commun.*, vol. 16, no. 6, pp. 3747–3760, 2017.

[13] D. W. K. Ng, E. S. Lo, and R. Schober, "Wireless information and power transfer: Energy efficiency optimization in OFDMA systems," *IEEE Trans. Wireless Commun.*, vol. 12, no. 12, pp. 6352–6370, 2013.

[14] C. Menini and F. V. Oystaeyen, *Abstract Algebra: A Comprehensive Treatment*, ser. Chapman & Hall/CRC Pure and Applied Mathematics. CRC Press, 2017.

[15] S. K. Zavriev and F. V. Kostyuk, "Heavy-ball method in nonconvex optimization problems," *Computational Mathematics and Modeling*, vol. 4, pp. 336–341, 1993.